Cooperative Hybrid VLC/RF Systems with SLIPT

Yue Xiao, Panagiotis D. Diamantoulakis, *Senior Member, IEEE,* Zequn Fang, Li Hao, *Member, IEEE,* Zheng Ma, *Member, IEEE* and George K. Karagiannidis, *Fellow, IEEE*

***Abstract*—A hybrid downlink system that simultaneously uses visible light communication (VLC) and radio frequency (RF) is investigated, assuming that only one of the two considered users is capable of receiving information over the optical band. In order to facilitate information transmissions from the VLC access point to the RF user, mixed VLC/RF relaying and simultaneous lightwave information and power transfer (SLIPT) are utilized. Moreover, a cognitive-based resource allocation policy and tractable bounds for the harvested energy are introduced. Furthermore, by taking into account the random location of the VLC and RF user terminals, the closed-form outage probability for the VLC user is given, while for the RF user, the outage probability is derived in terms of infinite-series, which is also approximated by a tractable closed-form expression. In addition, the outage probability of the RF user is minimized by optimizing the direct current (DC) component. Finally, simulations are provided to verify the accuracy of the theoretical analysis and demonstrate the effectiveness of the proposed optimization framework.**

***Index Terms*—Hybrid VLC/RF, cooperative relaying, cognitive based, simultaneous lightwave information and power transfer (SLIPT), outage probability, direct current (DC) component optimization.**

I. Introduction

In order to meet the tremendous wireless traffic growth and the demands for reduced latency, high energy saving, cost reduction, massive device connectivity and increased data rates, the design of wireless networks beyond the fifth generation (5G) has already attracted the research interest of both academia and industry, while several key technologies have been explored [1], such as network ultra-densification, interference management, and full-duplex. Nevertheless, conveying an exponentially increasing amount of data to the end users within an acceptable latency will inevitably lead to severe congestion of the RF spectrum. Therefore, spectrum expansion is a key technology to meet the aforementioned requirements [2].

A. State-of-the-Art & Motivation

Visible light communication (VLC) is a promising technology to tackle the forthcoming spectrum crunch. Its main advantages include the wide spectral availability and easy bandwidth reuse [3], [4]. In addition, due to the different frequency occupied by the visible and RF bands, there is no interference between VLC systems and radio frequency (RF) ones. Moreover, VLC is a green communication technology, since the illumination system can also be used for communications [5]. Recognizing the potential of this emerging technology, the Institute of Electrical and Electronic Engineers introduced the IEEE Standard 802.15.7, which was approved in June 2011 and has defined the physical layer (PHY) and medium access control (MAC) layer for VLC [6], [7]. However, the point-to-point VLC channel is sensitive to the blocking and shadowing effects due to the strict conditions required for the line-of-sight (LOS) transmissions, as such, VLC provides reduced wireless coverage compared to the conventional RF communication.

Although VLC is not expected to fully substitute the ubiquitous RF network, it is a promising and efficient complementary technology [8]. As a result, a heterogeneous network that uses both RF and VLC can be exploited by capitalizing on the benefits from both technologies. To this point, it is evident that the hybrid VLC/RF network can provide high system capacity, as well as the increased coverage. Therefore, several works have focused on the investigation of hybrid VLC-RF system's performance [9]–[13]. For example, the data rate of dual-hop VLC/RF communication system has been investigated in [9], while the outage performance of the cooperative VLC/RF system has been presented in [10]. Also, the authors in [11] have investigated the power allocation in the backhaul network consisting of hybrid VLC/RF scenario. Moreover, a user grouping method has been proposed in [12] to improve the data rate of the hybrid system. Furthermore, in [13], a novel cross-band selection combining method for a two-user hybrid lightwave/RF cooperative network with non-orthogonal multiple access (NOMA) mechanism has been investigated. It deserves to be noted that the upcoming co-existence of VLC and RF-based local area networks has also been taken into account by the IEEE 802.11 Working Group, leading to the creation of the 802.11bb Task Group on Light Communications in July 2018, which focuses on introducing necessary changes to the base IEEE 802.11 Standards to enable communications in the light medium [14].

Although the co-existence of VLC and RF can be explored to mitigate the LOS blockages and extend the coverage area, an important challenge associated with the hybrid VLC/RF wireless system is the conscious utilization of the available resources and the increase of energy sustainability. This challenge can be addressed, by using simultaneous lightwave information and power transfer (SLIPT), which was introduced in [15]–[17], where several enabling techniques were also proposed. By exploiting the intensity modulation-direct detection (IM-DD) scheme at the transceivers over the VLC channel

Y. Xiao, Z. Fang, and L. Hao, Z. Ma are with the Provincial Key Lab of Information Coding and Transmission, Southwest Jiaotong University, Chengdu 610031, China (e-mails: alice_xiaoyue @hotmail.com; {fangzequn, lhao, zma}@home.swjtu.edu.cn).

P. D. Diamantoulakis and George K. Karagiannidis are with the Electrical and Computer Engineering Department, Aristotle University of Thessaloniki, Thessaloniki 54124, Greece, and also with the Provincial Key Lab of Information Coding and Transmission, Southwest Jiaotong University, Chengdu 610031, China (e-mails: padiaman@ieee.org; geokarag@auth.gr).

[9], the irradiation of the optical wave can be modulated to carry the RF signal, while, an appropriate optical receiver can simultaneously decode the information and harvest energy from the alternate current (AC) and direct current (DC) components of the received optical signal, respectively [18]–[20]. It is noted that although RF-based wireless power transfer is a well investigated topic in the last ten years [21], [22], optical wireless power transfer is a new topic and only a few works have been reported so far in the open literature. Despite their differences mainly due to the utilized hardware, divergent channels' characteristics, and energy harvesting model, both technologies create an interesting trade-off between the communication rate and the harvested energy. Among the potential applications, SLIPT is particularly interesting for mixed VLC/RF cooperative networks, since the relay can use the harvested energy to forward the RF user's message without using its battery, as presented in [8], [9], [15], [23]–[26]. To this end, in [9], the selection of the DC bias was optimized with the aim to maximize the average data rate of the RF user, by utilizing a loose bound for the energy harvested at the relay. Moreover, the study in [15] contributed to narrowing the range of the optimal DC bias. Also in [23], the package loss probability for the RF user has been investigated, taking into account the end-to-end delay constraint. The secrecy outage probability of a hybrid VLC/RF network with energy harvesting has been presented in [24]. In [25], the achievable rate region of a cooperative VLC/RF system with an energy harvesting relay was explored. In addition, various receiver architectures enabling the SLIPT in VLC/RF systems were introduced in [8]. A hybrid RF/VLC ultra small cell network with SLIPT has been investigated in [26], with multiple angle-diversity transmitters having been considered.

However, to the best of the authors' knowledge, regarding hybrid VLC/RF systems with randomly deployed users, the optimization of the harvested energy and the investigation of the system's performance have not been performed yet in existing literature. Finally, it is highlighted that the concept of cognitive radio (CR) can also be utilized to further alleviate the spectrum scarcity and improve the spectrum utilization efficiency, according to which the primary users allow the secondary users to access their licensed spectrum bands in an opportunistic manner [27]. Based on the type of available network side information and the regulatory constraints, cognitive radio systems seek to underlay, overlay, or interweave their signals with those of existing users without significantly impacting their communication [28], [29]. To this point, it is noted that CR can be employed in conjunction with optical wireless networks to achieve higher area spectral efficiency [30]. Towards enhancing the network throughput of the hybrid free space optical (FSO)/RF cooperative network, the underlay cognitive radio inspired multiple-input multiple-output (MIMO) system has been investigated in [31].

B. Contribution

In this paper, a cognitive-based VLC/RF system with SLIPT is introduced, in which the VLC and RF frequency resources can be used in parallel to serve the involved users. More specifically, a cognitive-based resource allocation is proposed to be employed over the VLC link, such as to enable the information transmission from the VLC user to an RF one, who cannot directly receive the information emitted from the VLC access point (AP), without affecting the required quality-of-service (QoS) of the VLC user. Taking into account the randomness of users' locations, the performance of the proposed system is evaluated in terms of outage probability and optimized, providing tractable expressions. In more detail, the main contributions of this work can be summarized as follows:

- A cognitive-based policy for cooperative VLC/RF systems with SLIPT is proposed, according to which, adaptive resource allocation is performed at the VLC AP with the aim to preserve the rate requirement of the VLC user while leaving the surplus of resources for the RF user. Also, in order to avoid the reduction of the VLC user's battery lifetime and the degradation of its QoS, it is assumed that the VLC user solely exploits the harvested energy to perform relaying.
- We investigate the performance of the proposed system in terms of outage probability, taking into account that both users are randomly deployed. To this end, the outage probability of the VLC user is derived in closed-from, while a tractable approximation for the harvested energy is introduced, which is then used to derive an infinite-series expression for the outage probability of RF user. Although it is proven that the infinite-series expression converges with finite number or terms, which is investigated among others in the simulation results, a tractable closed-form approximation is also derived.
- An optimization framework is developed to facilitate the improvement of the system's outage performance. Specifically, within the context of the proposed cognitive-based resource allocation, the DC bias splitting parameter is optimized to improve the outage performance for the RF user without reducing the performance of the VLC user.
- Finally, simulation results are provided which verify the analysis, illustrate the effectiveness of the proposed system and optimization framework, and provide useful insights on the system's performance.

C. Structure

In what follows, the system model for this cognitive-based hybrid VLC/RF cooperative system is introduced in Section II. In Section III, the users' outage probability is investigated, considering the proposed cognitive-based resource allocation policy and the approximate harvested energy. To improve the system's performance, the SLIPT optimization is explored in Section IV, according to which, a suboptimal closed-form solution for the DC bias is derived to minimize the outage probability for the RF user while satisfying the requirement of the VLC user. Moreover, simulation results are presented in Section V, to demonstrate the accuracy of the analysis and the effectiveness of the proposed schemes. Finally, conclusions are summarized in Section VI.

This article has been accepted for publication in a future issue of this journal, but has not been fully edited. Content may change prior to final publication. Citation information: DOI 10.1109/TCOMM.2021.3051908, IEEE Transactions on Communications

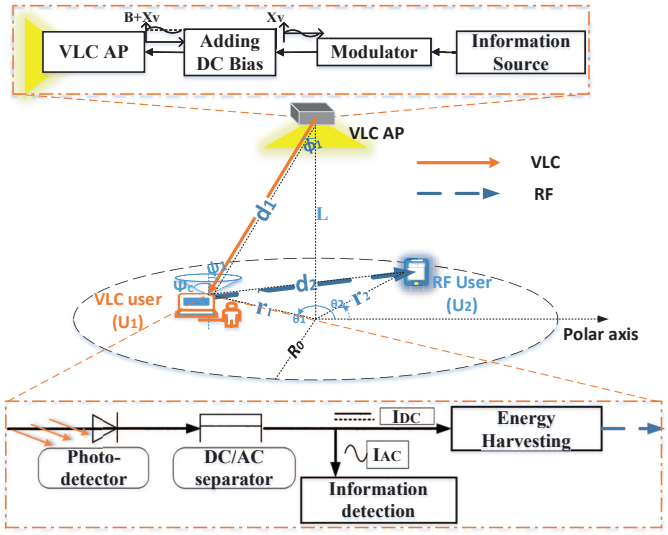

Fig. 1: System model of downlink relaying system with SLIPT.

II. System Model

An indoor downlink system is considered, consisting of one VLC AP and two users denoted by U_1 and U_2 respectively, with both being uniformly distributed in a disc with radius R_0, as shown in Fig. 1. Taking into account the user which is not capable of receiving direct transmission or not well served from the VLC AP, e.g., the terminal who has no photo-detector (PD), the transmission meets severe line-of-sight blockage, etc. [32], U_1 is considered as the VLC user (i.e., the user equipped with PD), while U_2 is viewed as the RF user hereinafter. Moreover, we assume that there is no direct optical link between the VLC AP and the RF user U_2.

It is assumed that the VLC AP transmits both users' message, e.g., by using time division duplexing (TDD), while U_1 receives its message directly from the VLC AP. Also, in order to facilitate the information transmission from the VLC AP to U_2, U_1 also acts as a relay, using mixed VLC/RF decode-and-forward (DF) relaying protocol. Also, considering that VLC is transparent to the communication at the RF band, U_1 operates in full-duplex mode. By using the polar coordinate system and the projection of the VLC AP at the users' plane as the reference point, the users' positions are defined by (r_i, θ_i), with r_i and θ_i being the radial and angular coordinate, respectively.

Considering the random deployment of the users, the corresponding angular coordinate follows the uniform distribution on the range of $\theta_i \in [0, 2\pi]$, thus the corresponding probability density function (PDF) can be expressed referring to [13], [32], and [33], given by

$$f_{\Theta_i}(\theta_i) = \frac{1}{2\pi} \ (\theta_i \in [0, 2\pi]). \tag{1}$$

For the radial coordinate, its PDF can be determined by differentiating the cumulative distribution function (CDF) over the radial variable r_i, in which the CDF can be explained as the ratio of corresponding areas, i.e., $F(r_i) = \frac{\pi r^2}{\pi R_0^2}$ [13]. Thus the PDF of $r_i \in [0, R_0]$ can be given by [13], [32], and [33], shown as

$$f_{\gamma_i}(r_i) = \frac{dF(r_i)}{dr_i} = \frac{2r_i}{R_0^2} \ (r_i \in [0, R_0]). \tag{2}$$

Furthermore, let L denote the vertical height of the VLC AP, thus the Euclidean distance between the VLC AP and U_1 can be expressed as

$$d_1 = \sqrt{r_1^2 + L^2}. \tag{3}$$

For calculating the distance between U_1 and U_2, the law of cosines can be exploited, thus we have [32]

$$d_2 = \sqrt{r_1^2 + r_2^2 - 2r_1 r_2 \cos(\theta_2 - \theta_1)}. \tag{4}$$

A. SLIPT over the VLC Link

Considering LoS and taking into account the polar coordinates system, the channel gain from the VLC AP to the VLC user is given by [34]

$$h_1 = \frac{C(s+1)L^{(s+1)}}{(r_1^2 + L^2)^{\frac{s+3}{2}}}, \tag{5}$$

where $C = \frac{A_r F(\psi_1) g(\psi_1)}{2\pi}$, A_r is the detection area of the photo detector (PD) at U_1, ϕ_1 and ψ_1 are the irradiate and incidence angles with the assumption of $\phi_1 \approx \psi_1$, s is the order of Lambertian by defining as $s = -\ln 2 / \ln(\cos \Phi_{1/2})$ with $\Phi_{1/2}$ being the transmitter semi-angle [35]. Besides, $F(\psi_1)$ and $g(\psi_1)$ are defined as the gains of the optical filter and optical concentrator respectively, with the latter being given by [35]

$$g(\psi_1) = \begin{cases} \frac{n^2}{\sin^2 \Psi_C} & , 0 \le \psi_1 \le \Psi_C, \\ 0 & , \psi_1 > \Psi_C, \end{cases} \tag{6}$$

with Ψ_C being the filed of view and n is an internal refractive index. Moreover, while considering the constraints of r_1, (5) can be bounded $[h_{1,\min}, h_{1,\max}]$, where

$$h_{1,\min} = \frac{C(s+1)L^{(s+1)}}{(R_0^2 + L^2)^{\frac{s+3}{2}}}, \quad h_{1,\max} = \frac{C(s+1)}{L^2}. \tag{7}$$

As shown in Fig.1, the non-negativity of the transmitted optical signal can be assured by adding a DC bias to the modulated signal, i.e., $x_v = x_m + \mathcal{B}$, where $\mathcal{B}$ is the direct current (DC) bias. In more detail, the electrical signal x_m varies in $\mathcal{B} \in [I_L, I_H]$ with the corresponding peak amplitude $\mathcal{A}$, with I_L and I_H being the minimum and maximum input bias current, respectively, i.e., $\mathcal{A} \le \min(\mathcal{B} - I_L, I_H - \mathcal{B})$ [15]. Moreover, two auxiliary variables are introduced to rewrite above DC/AC constraints in a more compact form, i.e., a splitting parameter for DC bias $\rho \in [0, 1]$ and another with respect to the peak amplitude component $\rho_{\mathcal{A}}$, thus we have

$$\mathcal{B} = I_L + \rho(I_H - I_L), \tag{8}$$

$$\mathcal{A} \le \rho_A (I_H - I_L), \tag{9}$$

where $\rho_{\mathcal{A}} = \min(\rho, 1 - \rho)$. Accordingly, the output of PD at U_1 can be rewritten as

$$y_1 = I_{DC} + I_{AC} + n_1, \tag{10}$$

with $I_{\rm AC} = \eta h_1 P_1 \mathcal{A} x_{\rm m}$ and $I_{\rm DC} = \eta h_1 P_1 \mathcal{B}$ being the alternating current (AC) and DC component, respectively, which can be obtained through the DC/AC separator consists of diode and capacitor. P_1 is the optical power from the VLC AP (in W/A). Moreover, η is the PD responsivity in A/W, $n_1 \sim \mathcal{CN}(0, \delta_1^2)$ is the additive white Gaussian noise (AWGN). By considering the coefficients given in (8) and (9), the AC and DC components can be further derived as

$$I_{AC} = \rho_{\rm A} \eta h_1 P_1 (I_H - I_L) x_{\rm m} \tag{11}$$

and

$$I_{DC} = \eta h_1 P_1 \left(\rho I_H + (1-\rho) I_L\right), \tag{12}$$

respectively. Thus by leveraging the AC and DC components, users have the capability to gather information and energy simultaneously.

Assuming the use of intensity-modulation direct-detection (IM/DD), the lower bound of the achievable rate in the VLC link is given by [36]

$$\mathcal{R}_1 = B_{\rm v} \log_2 \left(1 + \tfrac{e(\eta h_1 P_1 \mathcal{A})^2}{2\pi\sigma_1^2}\right), \tag{13}$$

with $B_{\rm v}$ being the bandwidth of the VLC system. Furthermore, the achievable rate of the dedicated information to U_1 and $\rm U_2$ can be expressed as

$$\mathcal{R}_{1,i} = \alpha_i \mathcal{R}_1, \tag{14}$$

where $\alpha_i (i \in \{1,2\})$ is the ratio of the achievable rate for the considered user to the sum capacity, constrained by $0 \leq \alpha_i \leq 1, \forall i \in \{1,2\}$ and $\alpha_1 + \alpha_2 \leqslant 1$.

It is noteworthy that when TDD is used, $\alpha_i (i \in \{1,2\})$ correspond to the time allocation parameters. Thus during a unit time period (i.e., $\alpha_1 + \alpha_2$), the energy harvested at $\rm U_1$ can be expressed as

$$E_{\rm h,1} = f \eta h_1 P_1 \mathcal{B} V_{\rm t} \ln \left(1 + \frac{\eta h_1 P_1 \mathcal{B}}{I_0}\right), \tag{15}$$

where f is the fill factor which is defined as the ratio of maximum generated power to the theoretical power. In practice, the fill factor receives values between 0.7 to 0.8 [37]. $V_{\rm t}$ is the thermal voltage and I_0 is the dark saturation current [15]. Thus, by focusing on a single time slot herein, the unit of the harvested energy can be denoted by joule per second (i.e., watt).

B. Transmissions over the RF Link

Assuming that the energy for data detection and reception at $\rm U_1$ is neglected, the energy harvesting at $\rm U_1$ during the normalized time period $(\alpha_1 + \alpha_2)$ is used for data (i.e., x_2) retransmission from $\rm U_1$ to $\rm U_2$. Considering the harvested energy given by (15), the received signal by $\rm U_2$ can be written as

$$y_2 = \sqrt{E_{\rm h,1}} x_2 h_2 + n_2, \tag{16}$$

where h_2 denotes the Rcian fading channel and $n_2 \sim \mathcal{CN}(0, \delta_2^2)$ is the corresponding AWGN noise, x_2 is the retransmitted electrical signal with normalized power, i.e., $\mathbb{E}(|x_2|^2) = 1$.

Accordingly, the achievable data rate in the RF subsystem can be directly given by the Shannon formula as

$$\mathcal{R}_2 = B_{\rm r} \log_2 \left(1 + \frac{E_{\rm h,1} |h_2|^2}{G_{\rm R} \sigma_2^2}\right), \tag{17}$$

where $B_{\rm r}$ is the bandwidth for the RF system, $G_{\rm R} = (\frac{4\pi d_0}{\lambda})^2 (\frac{d_2}{d_0})^v$ is the path loss parameter with λ and v being the corresponding carrier wavelength and the path loss exponent, respectively, and d_0 is the reference distance [9]. Notably, all the energy harvested within a normalized time duration via the VLC link is then leveraged for the information retransmission via the RF link. Inspired by the relaying strategy of decode-and-forward, the end-to-end capacity of $\rm U_2$ is dominated by the weakest link among the VLC link and RF link. Accordingly, the achievable data rate of $\rm U_2$, i.e. $\mathcal{R}_2^{E2E}$, in this cooperative VLC/RF system can be expressed as

$$\mathcal{R}_2^{E2E} = \min\left(\mathcal{R}_{1,2}, \mathcal{R}_2\right). \tag{18}$$

III. Resource Allocation and Performance Analysis

In this section, a cognitive-based resource allocation policy and tractable bounds of the harvested energy by $\rm U_2$ are introduced, which are then used to investigate the performance analysis of the proposed system in terms of outage probability.

c

A. A Cognitive-based Resource Allocation Policy

Assuming that the channel gain between the VLC AP and $\rm U_1$ is known at the VLC AP, the aim of the proposed cognitive-based resource allocation policy is to serve the RF user without creating a burden to the VLC user that also acts as a relay. This can be achieved by adaptively setting α_1 and α_2 with respect to h_1, such as to guarantee that the difference between the achieved $(\mathcal{R}_{1,1})$ and the target rate $(\rm R_{th,1})$ for the VLC user is minimum and the available resources are not underutilized. More specifically, the RF user is served only if $\mathcal{R}_{1,1} = \rm R_{th,1}$ for $\alpha_1 \leq 1$. Thus, considering (14), the optimal values of α_i $(i = 1, 2)$ are given by

$$\alpha_1^* = \frac{\rm R_{th,1}}{B_{\rm v} \log_2 (1 + \frac{e(\eta h_1 P_1 \mathcal{A})^2}{2\pi\sigma_1^2})} \tag{19}$$

and

$$\alpha_2^* = \begin{cases} 1 - \alpha_1^*, & 0 \leqslant \alpha_1^* \leqslant 1, \\ 0, & \alpha_1^* > 1, \end{cases} \tag{20}$$

respectively.

B. An Approximation for the Harvested Energy

To facilitate the performance analysis, a tractable format of the harvested energy shall be investigated. As it is observed by (15), the logarithmic term in (15) complicates the mathematical analysis of the harvested energy [9]. To this point, a tight approximation of the $E_{\rm h,1}$ shall be provided in the following. First, a closer look at (15) reveals that the energy harvested by $\rm U_1$ depends on the optical channel gain (i.e., h_1), which can be further equivalently rewritten as a function related to different

This article has been accepted for publication in a future issue of this journal, but has not been fully edited. Content may change prior to final publication. Citation information: DOI 10.1109/TCOMM.2021.3051908, IEEE Transactions on Communications

locations of U_1 after observing the optical channel gain given in (5) and its corresponding bounds (7). By plugging (7) into the logarithmic term of (15) and referring to the monotone feature held by the logarithm $\ln(.)$, we can further derive that

$$f\eta h_1 P_1 \mathcal{B} V_{\mathrm{t}} \ln\left(1+\frac{\eta h_{1,\min} P_1 \mathcal{B}}{I_0}\right) \leq E_{\mathrm{h},1}^{\mathrm{app}*} \leq f\eta h_1 P_1 \mathcal{B} V_{\mathrm{t}} \ln\left(1+\frac{\eta h_{1,\max} P_1 \mathcal{B}}{I_0}\right). \tag{21}$$

Furthermore, by introducing an auxiliary variable $\beta \in [0,1]$, the above inequality (21) can be equivalently rewritten in a more compact form, given by

$$E_{\mathrm{h},1}^{\mathrm{app}*} = f\eta h_1 P_1 \mathcal{B} V_{\mathrm{t}} \mathcal{W}_{\mathrm{oc}}, \tag{22}$$

where

$$\mathcal{W}_{\mathrm{oc}} = [\beta \ln(1+\frac{\eta h_{1,\max} P_1 \mathcal{B}}{I_0}) + (1-\beta)\ln(1+\frac{\eta h_{1,\min} P_1 \mathcal{B}}{I_0})]. \tag{23}$$

With given other parameters, $\beta = \{1, 0\}$ corresponds to the upper and lower bound of the harvested energy, respectively. The tightness of the expected performance by using the proposed approximation is investigated in Section V.

C. Outage Probability

Next, we derive the outage probability of user U_i, which is defined as the probability that the achieved rate falls below a predefined threshold $R_{\mathrm{th},i}$. Specifically, the outage probability for decoding the information x_i at U_1 can be expressed as

$$\mathrm{P}_{1,\mathrm{i}}^{\mathrm{O}} = \mathrm{P}_{\mathrm{r}}[\mathcal{R}_{1,i} < \mathrm{R}_{\mathrm{th},i}]. \tag{24}$$

By considering data rates $\mathcal{R}_{1,i}$ as given in (14) and the service priority required by U_1 as stated in Section III-A, it is noted that the baseline scheme with random resource allocation cannot achieve higher data rate for decoding x_2 at the VLC link, while also meeting the target rate for information x_1 first, or even results in worse performance. This is because, the splitting parameter for x_1 shall be designed first, to meet the target rate of U_1, then the spared resource is spent to the transmission of x_2 via the VLC link, or otherwise it will cause a waste of resources. Accordingly, the exact expressions are presented in the following theorem.

Theorem 1. *The outage probability that corresponds to the decoding of x_i by U_1 via the VLC link can be expressed in closed form, as*

$$\mathrm{P}_{1,\mathrm{i}}^{\mathrm{O}} = 1 - \frac{\left((C(s+1)L^{(s+1)})^2/\zeta_{1,\mathrm{i}}^*\right)^{\frac{1}{3+s}} - L^2}{R_0^2}, \tag{25}$$

where

$$\zeta_{1,\mathrm{i}}^* = \min\{\max\{\zeta_{1,\mathrm{i}}, Y_{1,\min}\}, Y_{1,\max}\}, \tag{26a}$$

$$\zeta_{1,1} = \frac{2\pi\sigma_1^2(2^{\frac{\mathrm{R}_{\mathrm{th},1}}{B_{\mathrm{v}}}}-1)}{e(\eta P_1 \mathcal{A})^2}, \tag{26b}$$

$$\zeta_{1,2} = \frac{2\pi\sigma_1^2(2^{\frac{(\mathrm{R}_{\mathrm{th},1}+\mathrm{R}_{\mathrm{th},2})}{B_{\mathrm{v}}}}-1)}{e(\eta P_1 \mathcal{A})^2}, \tag{26c}$$

$$[Y_{1,\min}, Y_{1,\max}] = \Big[\frac{(C(s+1)L^{(s+1)})^2}{(R_0^2+L^2)^{(s+3)}}, \frac{(C(s+1)L^{(s+1)})^2}{L^{2(s+3)}}\Big]. \tag{26d}$$

Proof: Considering the proposed cognitive-based resource allocation policy, the VLC user is served in priority and the service to RF user is only activated if $\mathcal{R}_{1,1} = \mathrm{R}_{\mathrm{th},1}$ when $\alpha_1 \leq 1$, as mentioned in Section III-A. In regard to the outage probability for decoding information x_1 of U_1, we have

$$\mathrm{P}_{1,1}^{\mathrm{O}} = \mathrm{P}_{\mathrm{r}}[\mathcal{R}_{1,1} < \mathrm{R}_{\mathrm{th},1}] \overset{(a)}{=} \mathrm{P}_{\mathrm{r}}[\alpha_1^* > \alpha_1] \overset{(b)}{=} \mathrm{P}_{\mathrm{r}}\left[\alpha_1^* > 1\right] = \mathrm{P}_{\mathrm{r}}\left[|h_1|^2 < \zeta_{1,1}^*\right], \tag{27}$$

where step (a) is established after some manipulations and by substituting (19) into the derivation, step (b) follows the case that the outage event for U_1 only occurs when $\alpha_1^* > \max(\{\alpha_1\})$. Subsequently, for decoding information x_2 at U_1, we have

$$\mathrm{P}_{1,2}^{\mathrm{O}} = \mathrm{P}_{\mathrm{r}}[\mathcal{R}_{1,2} < \mathrm{R}_{\mathrm{th},2}] \overset{(c)}{=} \mathrm{P}_{\mathrm{r}}[\alpha_2^* \mathcal{R}_1 < \mathrm{R}_{\mathrm{th},2}] = \mathrm{P}_{\mathrm{r}}\left[|h_1|^2 < \zeta_{1,2}^*\right], \tag{28}$$

where step (c) follows the cognitive-based policy as given in (19) and (20). Then, after plugging (19) into this term, we can derive $\zeta_{1,2}^*$ as shown in (26c). Furthermore, by substituting (5) into the above (27) and (28), we have

$$\mathrm{P}_{\mathrm{r}}\left[|h_1|^2 < \zeta_{1,\mathrm{i}}^*\right] = \Pr\left[\frac{(C(s+1)L^{(s+1)})^2}{(r_1^2+L^2)^{s+3}} < \zeta_{1,i}^*\right] = 1 - \Pr\left[r_1 < r_{1,\mathrm{i}}^c\right], \tag{29}$$

where

$$r_{1,\mathrm{i}}^c = \sqrt{\left((C(s+1)L^{(s+1)})^2/\zeta_{1,\mathrm{i}}^*\right)^{\frac{1}{3+s}} - L^2}. \tag{30}$$

To this end, we can further derive (29) in closed-form by using the cumulative distribution function (CDF) of r_i, i.e. $F_{\gamma_\mathrm{i}}(r_i) = \frac{r_i^2}{R_0^2}(r_i \in [0, R_0])$ [32], then the proof is completed. □

It is noted that the outage probability for U_1 can be directly given by (25), for $i = 1$.

Due to the DF relaying protocol assumed in this mixed dual-hop system, the outage event for U_2 is determined by both the VLC and RF link. Thus, the outage probability of U_2 can be denoted as

$$\mathrm{P}_2^{\mathrm{O}} = \mathrm{P}_{\mathrm{r}}[\mathcal{R}_{1,2} < \mathrm{R}_{\mathrm{th},2}] + \mathrm{P}_{\mathrm{r}}[\mathcal{R}_{1,2} > \mathrm{R}_{\mathrm{th},2} \cap \mathcal{R}_2 < \mathrm{R}_{\mathrm{th},2}], \tag{31}$$

with the first term being the outage event for decoding x_2 at U_1, while the case corresponding to the successful receiving at U_1 but fails at U_2 is considered as the second term. Towards this, further observations are included in the following theorems.

Theorem 2. *An infinite-series approximation to the outage probability for the user U_2 can be expressed as in (32), at the top of the next page, where*

$$M = 2l + \frac{(n+1)v}{2} - p + 2q + 2, \tag{33}$$

$$\mathrm{P}_2^{\mathrm{O,app}} = 1 - \frac{\left((C(s+1)L^{(s+1)})^2/\zeta_{1,2}^*\right)^{\frac{1}{3+s}} - L^2}{R_0^2} + \exp(-K)\sum_{n=0}^{\infty}\frac{(-1)^n}{\pi^2 R_0^4}\frac{L_{\mathrm{n}}^{(0)}(K)}{\Gamma(n+2)}\left(\frac{(1+K)\Lambda_c^*}{\Omega}\right)^{(n+1)}\sum_{p=0}^{\frac{(n+1)v}{2}}\sum_{l=0}^{p}$$
$$\sum_{q=0}^{\frac{(n+1)(s+3)}{2}}\binom{\frac{(n+1)v}{2}}{p}\binom{p}{l}\binom{\frac{(n+1)(s+3)}{2}}{q}(-2)^{(\frac{(n+1)v}{2}-p)}L^{((n+1)(s+3)-2q)}\left(\frac{(r_{1,2}^c)^M R_0^N}{MN}\right)\sum_{k=0}^{\frac{(n+1)v}{2}-p}\binom{\frac{(n+1)v}{2}-p}{k}$$
$$(-1)^{\frac{(n+1)v}{2}-p-k}\mathcal{J}^2. \tag{32}$$

$$N = p - 2l + \frac{(n+1)v}{2} + 2, \tag{34}$$

and

$$\mathcal{J} = \frac{1}{2}B\left(\frac{\frac{(n+1)v}{2}-p-k+1}{2}, \frac{k+1}{2}\right) \times \left(1+(-1)^{\frac{(n+1)v}{2}-p-k}\right)\left(1+(-1)^k\right), \tag{35}$$

with $B(x,y)$ being the beta function [38]. K is the Rician factor, Ω is the variance of the transmitted signal, $\Gamma(.)$ denotes the Euler gamma function, and $L_{\mathrm{n}}^{(0)}(.)$ stands for the generalized Laguerre polynomial of degree n and order 0.

Proof: Please refer to Appendix A. □

As it has been proved in [39], the series in (32) converges and provides acceptable accuracy by only using few terms, the number of which is denoted by N_m, as verified by the simulation in Section V. Furthermore, in order to obtain more insights on the system's performance in terms of outage probability, a tractable closed-form approximation is given in the following theorem, the accuracy of which is also validated in Section V.

Theorem 3. *A closed-form approximation for the outage probability of U_2 can be expressed as*

$$\mathrm{P}_2^{\mathrm{O,app(c)}} \approx 1 - \frac{\left(\left(C(s+1)L^{(s+1)}\right)^2/\zeta_{1,2}^*\right)^{\frac{1}{3+s}} - L^2}{R_0^2} + \sum_{p=0}^{\frac{(n+1)v}{2}}\binom{\frac{(n+1)v}{2}}{p}\left(\frac{(1+K)\Lambda_c^*}{\Omega}\right)\exp(-K)\frac{\Xi_r\Xi_\theta}{\pi^2 R_0^4}, \tag{36}$$

which is an accurate approximation of (32) when it holds that

$$\Lambda_c^*\left(r_1^2 + r_2^2 - 2r_1r_2\cos(\theta_2-\theta_1)\right)^{\frac{v}{2}}\left(r_1^2+L^2\right)^{\frac{(s+3)}{2}} \to 0^+. \tag{37}$$

Proof: Please see the detailed proof in Appendix B. □

IV. SLIPT Optimization

Considering the SLIPT-based VLC/RF system and the use of the cognitive-based resource allocation policy, a DC bias optimization is explored in this section. More specifically, the different functions of DC and AC motivate us to study the trade-off between the harvested power and the received SNR, leading to better QoS for the involved users, which can be achieved by adjusting the DC- and AC- bias splitting parameters (i.e., ρ and ρ_A).

Moreover, the priority of the VLC user considered in the proposed cognitive-based resource allocation policy as shown in Section III-A, is also be taken into account in the following optimization problem. In such case, the performance of U_1 that is achieved in this cognitive system in terms of outage probability is the best possible.

Proposition 1. *To guarantee the best outage performance of the VLC user U_1, and even prevent outage, the feasible splitting parameter (i.e., ρ and $\rho_{\mathcal{A}}$) can be decided by the following two cases:*

- *Case 1: If $\rho_{\mathcal{A},L} \leqslant 0.5$, we have*

$$\rho_{\mathcal{A},L} \leqslant \rho^* \leqslant 1 - \rho_{\mathcal{A},L}, \tag{38}$$

- *Case 2: If $\rho_{\mathcal{A},L} > 0.5$, we have*

$$\rho^* = 0.5, \tag{39}$$

with $\rho_{\mathcal{A},L}$ denoting the lower bound of the AC splitting coefficient $\rho_{\mathcal{A}}$, which can be specified by

$$\rho_{\mathcal{A},L} = \left[\frac{2\pi\sigma_1^2(2^{\frac{(\mathrm{R_{th,1}})}{B_\mathrm{v}}}-1)(R_0^2+L^2)^{(s+3)}}{e\left[\eta P_1 C(s+1)(I_\mathrm{H}-I_\mathrm{L})L^{(s+1)}\right]^2}\right]^{1/2}. \tag{40}$$

Notably, the case with $\rho_{\mathcal{A},L} > 0.5$ implies that it's impossible to achieve the non-outage status for the VLC user, i.e., $\mathrm{P}_{1,1}^{\mathrm{O}} \neq 0, \forall\rho \in [0,1]$.

Proof: The proof is given in Appendix C. □

Following the prioritization that considered in the proposed cognitive-based resource allocation policy, the optimization problem of the outage probability performed by the RF user (i.e., U_2) shall be constrained by the expressions that are given in Proposition 1. In what follows, focus on case 1 of Proposition 1, assuming that $\rho_{\mathcal{A},L} \leqslant 0.5$. To this point, the optimization problem for U_2 can be formulated as

$$\begin{aligned} &\min_{\rho}\ \mathrm{P}_2^{\mathrm{O}} \\ &\mathbf{s.t.}\ \mathrm{C}_1\ : \rho \in [\rho_{\mathcal{A},L}, 1-\rho_{\mathcal{A},L}] \qquad \rho_{\mathcal{A},L} \leqslant 0.5, \\ &\qquad \mathrm{C}_2\ : \rho \in [0,1], \end{aligned} \tag{41}$$

where $\mathrm{P}_2^{\mathrm{O}}$ is the outage probability of RF user as given by (46).

Moreover, a closer look at the outage probability $\mathrm{P}_2^{\mathrm{O}}$ with respect to the harvested energy $\mathrm{E_{h,1}}$ implies that, the optimization problem (41) without considering the constraint C_1, can

This article has been accepted for publication in a future issue of this journal, but has not been fully edited. Content may change prior to final publication. Citation information: DOI 10.1109/TCOMM.2021.3051908, IEEE Transactions on Communications

be directly transformed to finding the maximum value of $\mathrm{E_{h,1}}$ in terms of the optimal DC current. Then the constraint given in $\mathrm{C_1}$ is taken into account at the next stage of the solution. To this point, in the case where the outage probability of $\mathrm{U_2}$ without affecting by $\mathrm{U_1}$, the optimization problem (41) can be first reduced to

$$\begin{aligned} \max_{\mathcal{B}} \ & \mathrm{E_{h,1}} \\ \mathbf{s.t.}\ & \mathcal{A} \leqslant \min(\mathcal{B}-I_{\mathrm{L}}, I_{\mathrm{H}}-\mathcal{B}), \\ & \mathcal{A} \geqslant 0, \\ & \mathcal{B} \in [I_{\mathrm{L}}, I_{\mathrm{H}}]. \end{aligned} \tag{42}$$

Proposition 2. *To minimize the outage probability for the RF user (i.e.,* $\mathrm{U_2}$*) while considering the protocol of SLIPT, i.e., the energy harvested by* U_1 *(*$\mathrm{E_{h,1}}$*), the optimal DC bias* $\mathcal{B}$ *should be designed in the range of* $[\frac{I_L+I_H}{2}, I_H]$*, i.e., equivalently* $\rho^* \in [0.5, 1]$.

Proof: Referring to the energy harvested at $\mathrm{U_1}$, i.e., $\mathrm{E_{h,1}}$, as given by (15), we first assume that the optimal solution is $\mathcal{B}^* < \frac{I_L+I_H}{2}$, which satisfies all the other constraints. Then, following the proof by contradiction as in [15], larger $\mathrm{E_{h,1}}$ can be gained when $\mathcal{B} \geq \frac{I_L+I_H}{2}$, while it further increases with the increasing $\mathcal{B}$, which is equivalent to $\rho^* \in [0.5, 1]$. Consequently, Proposition 2 has been proved. □

Till now, it's still noteworthy that the harvested power in achieving the reliable information transmission from $\mathrm{U_1}$ to $\mathrm{U_2}$ shall be explored without diminishing the performance of $\mathrm{U_1}$. That is, the requirements of both cognitive policy and maximum harvested energy shall be taken into consideration on deciding the optimal SLIPT parameter. Thus, on the premise of the limitation of DC bias $\mathcal{B}$ (equivalently, the splitting parameter ρ) as given in Proposition 1 and 2, it's of interest to further explore the DC bias which leads to the minimized outage probability for $\mathrm{U_2}$, considering the reduced range of ρ^*. To this end, (41) can be rewritten as

$$\begin{aligned} \min_{\rho} \ & \mathrm{P_2^O} \\ \mathbf{s.t.}\ & \mathrm{C_1}, \mathrm{C_2^{'}} : \rho \in [0.5, 1]. \end{aligned} \tag{43}$$

Due to the form of the objective function, the optimal ρ cannot be directly derived in closed-form and can only be calculated by using and one-dimensional search algorithm. However, capitalizing on the above two propositions, a suboptimal but tractable solution for ρ can be derived by solely considering one of the two independent outage events, i.e., $\mathrm{P_{1,2}^O}$ and $\mathrm{P_{2,RF}^O}$, under specific conditions, which is provided in the following theorem.

Theorem 4. *Conditioned on satisfying the outage performance of the VLC user (*U_1*), the DC bias splitting parameter* ρ *leading to the minimized outage probability of the RF user (*U_2*) can be classified in the following two categories by leveraging the value given by (40), thus,*

1) *When* $\rho_{\mathcal{A},L} > 0.5$*, although outage for the VLC user cannot be avoided, i.e.,* $\mathrm{P_{1,1}^O} \neq 0$*, we have* $\rho^* = 0.5$ *to meet the best performance of the VLC user, as stated in case 2 of Proposition 1.*
2) *When* $\rho_{\mathcal{A},L} \leqslant 0.5$*, since that the non-outage status for the VLC user can be achieved as given in the case 1 of Proposition 1, thus the suboptimal solution to the minimum outage probability for* U_2 *can be expressed as*

$$\rho^* \approx \max\{0.5, \min(1, 1-\rho_{\mathcal{A}}^*)\}, \tag{44}$$

where

$$\rho_{\mathcal{A}}^* = \left[\frac{2\pi\sigma_1^2(2^{\frac{(\mathrm{R_{th,1}}+\mathrm{R_{th,2}})}{B_{\mathrm{v}}}}-1)(R_0^2+L^2)^{(s+3)}}{e\left[\eta P_1 C(s+1)(I_{\mathrm{H}}-I_{\mathrm{L}})L^{(s+1)}\right]^2}\right]^{1/2}. \tag{45}$$

Proof: Please refer to Appendix D. □

V. Simulation Results

In this section, Monte-Carlo simulations are performed to verify the accuracy of the Theorems 1-4 presented in Section III. We let $\gamma_{\mathrm{th},1} = (2^{\frac{\mathrm{R_{th,1}}}{B_{\mathrm{v}}}}-1)2\pi/e$ denote the normalized threshold value of U_1, while $\mathrm{U_2}$ holds the corresponding value as $\gamma_{\mathrm{th},2} = (2^{\frac{\mathrm{R_{th,2}}}{B_{\mathrm{r}}}}-1)$. As for the average value of the received SINR, we denote it as $\rho_{\mathrm{A}}^2\bar{\gamma}$, where $\bar{\gamma} = \frac{(\eta h_1 P_1 (I_H-I_L))^2}{\sigma_1^2}$. In what follows, for the sake of generality, the ratio $\bar{R} = \frac{\mathrm{R_{th,1}}/B_{\mathrm{v}}}{\mathrm{R_{th,2}}/B_{\mathrm{r}}}$ is used. Accordingly, with given specific values of the normalized SNR with respect to the target rate for $\mathrm{U_i}$, i.e., $\bar{\gamma}/\gamma_{\mathrm{th},1}$, and the ratio $\bar{R}$, it's intuitive to derive those for $\gamma_{\mathrm{th},1}$ and $\gamma_{\mathrm{th},2}$, which can be further leveraged to explore the performance for both users. Unless otherwise specified, the parameters' values are given in Table-I, while $\mathcal{A} = \frac{I_{\mathrm{H}}-I_{\mathrm{L}}}{2}$, $\mathcal{B} = \frac{I_{\mathrm{H}}+I_{\mathrm{L}}}{2}$ [15], equivalently $\rho = 0.5$.

TABLE I: Simulation parameters

Parameter	Value	Parameter	Value	Parameter	Value
R_0	3 m	L	3 m	A_{r}	1 cm^2
v	2	m	1	Ψ_{C}	60^o
n	1.5	f	0.7	$\Phi_{1/2}$	60^o
$F(\psi_{\mathrm{i}})$	1	K	2	η	0.75 A/W
I_{L}	0 mA	I_{H}	12 mA	I_0	10^{-9} A
λ	1.25	Ω	1	V_{t}	25 mA
P_1	20W/A	σ_1^2	9.3×10^{-16}[9]	σ_2^2	10^{-8}[9]

In Figs. 2 and 3, the average achievable rate for the RF user is plotted versus DC bias splitting parameter ρ and resource allocation splitting parameter α_2, respectively, with fixing the normalized SNR as $\bar{\gamma}/\gamma_{\mathrm{th},1} = 20$ dB and the ratio as $\bar{R} = 20$. The reason for this ratio setting is that VLC in general achieves higher spectral efficiency compared to the RF counterpart, let alone the fact that the RF transmission is solely based on the harvested energy. As depicted in Fig.2, the end-to-end achievable rate is plotted by comparing the diverse rates obtained from the VLC link and RF link, by referring to (18) given in Section.II. Therein, the separate rates obtained via the two links are denoted by $\mathrm{R^{VLC}(U_2)}$ and $\mathrm{R^{RF}(U_2)}$, respectively, in the figure. Meanwhile, in order to investigate more situations, the resource allocation splitting parameter is assumed as $\alpha_2 = \{0.2, 0.3, 0.5\}$. One can observe that the achievable rate of $\mathrm{U_2}$ obtained via the RF link is not affected by the resource allocation strategy, due to that the division of the sum capacity is only considered in the VLC link, as

This article has been accepted for publication in a future issue of this journal, but has not been fully edited. Content may change prior to final publication. Citation information: DOI 10.1109/TCOMM.2021.3051908, IEEE Transactions on Communications

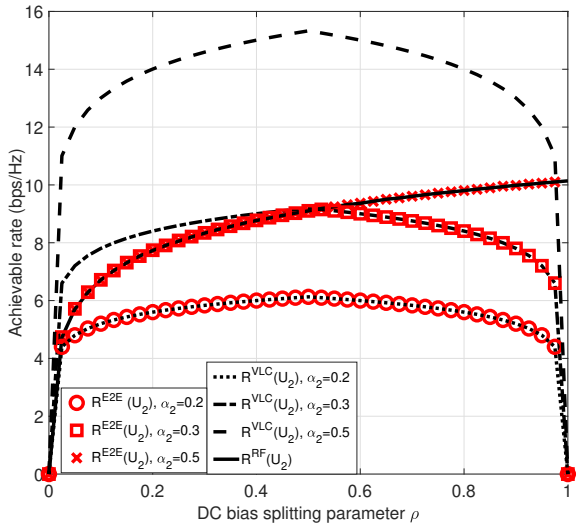

Fig. 2: Achievable rate of U_2 versus DC bias $\mathcal{B}$.

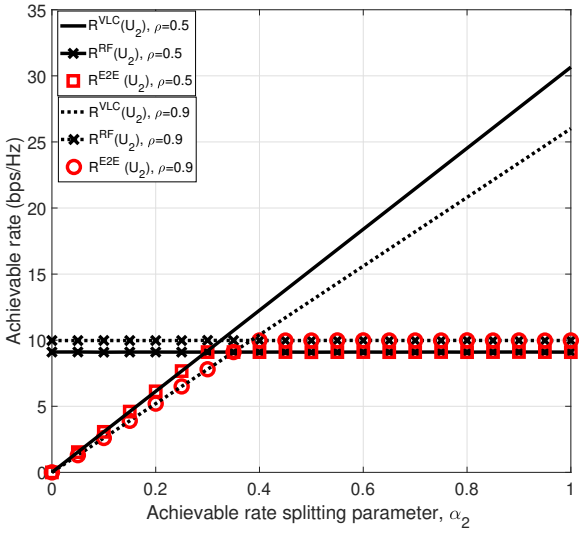

Fig. 3: Achievable rate of U_2 versus the resource allocation splitting parameter α_2.

stated in the above (14). On the other hand, we can find that the appropriate DC bias splitting parameter ρ can help to maximize the end-to-end achievable rate. Specifically, in order to obtain the maximized rate in Fig. 2, ρ can be set as $\rho = \{0.5, 0.5, 0.98\}$, corresponding to $\alpha_2 = \{0.2, 0.3, 0.5\}$, respectively. Similarly, while fixing the DC bias splitting parameter as $\rho = \{0.5, 0.9\}$ in Fig.3, the maximum end-to-end rate can be achieved by setting the resource allocation parameter as $\alpha_2 = \{0.3, 0.4\}$, respectively.

As presented in Fig. 4, the outage probability for each user is plotted versus different values of $\bar{\gamma}/\gamma_{\mathrm{th},1}$ with $\rho = 0.5$ for different values of the ratio, i.e., $\bar{R} = \{5, 10, 20\}$. The reason for this ratio setting is twofold: one is for the data achieved via the RF subsystem is strictly limited by the energy harvesting at the VLC link, the other is due to the larger bandwidth for VLC compared with the RF system, in practice. Recall to the approximation aforementioned in

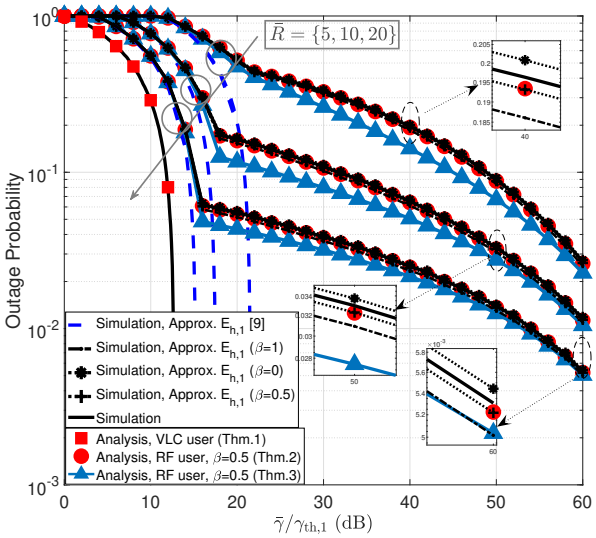

Fig. 4: Outage probability versus the normalized SNR $\bar{\gamma}/\gamma_{th,1}$(dB).

Section III-B, $\beta = \{0, 1\}$ correspond to upper and lower bounds of the outage probability of U_2, respectively, while $\beta = 0.5$ represents an approximate value in that range of the outage probability. For U_1, the closed-form analysis as given in Theorem 1 matches well with the simulation results. Meanwhile, one can observe that all the three different parameter settings for U_1 share the same outage performance, due to the usage of the same normalized SNR (i.e., $\bar{\gamma}/\gamma_{\mathrm{th},1}$). Regarding to U_2, the analytic approximation solutions of U_2 (i.e., Theorem 2 and 3) generally match well with the curves obtained from the simulations when $\beta = 0.5$, especially with the increase of the normalized SNR. Moreover, as the normalized SNR increases, one can also observe that the slopes of the curves drastically change after a value of the normalized SNR. This is due to the cognitive-based resource allocation policy considered at U_1, according to which the VLC user is in higher priority, while its outage probability reaches to 0 after the aforementioned value of SNR. More specifically, as shown in Fig. 4, Theorem 2 can provide more accurate results in comparison with that of Theorem 3, which is at the expense of the complexity of the calculation as shown in (32). Moreover, it is noted that the number of terms that are required for the convergence of the infinite series-based expression for the outage probability in Theorem 2 is acceptable, i.e., $N_{\mathrm{m}} = \{51, 18, 14\}$ for $\bar{R} = \{5, 10, 20\}$, respectively. For the Theorem 3, it is noted that there is no big performance deviation compared with the simulation results, especially for the higher normalized SNR and bigger values of the rate ratio, which are accordance with the approximation analysis in Section III-Theorem 3. Overall, compared with the upper-bounded of harvested energy (i.e., $E_{\mathrm{h},1}$) used in [9], i.e., $E_{\mathrm{h},1}^{[9]} = \frac{f(\eta h_1 P_1 \mathcal{B})^2 V_{\mathrm{t}}}{I_0}$, the proposed solutions in (22) can obviously improve the accuracy of performance analysis.

To figure out the impact of the DC bias on the system's performance, we plot the outage probability for both users versus the DC bias splitting parameter $\rho \in [0, 1]$ in Fig. 5, with

This article has been accepted for publication in a future issue of this journal, but has not been fully edited. Content may change prior to final publication. Citation information: DOI 10.1109/TCOMM.2021.3051908, IEEE Transactions on Communications

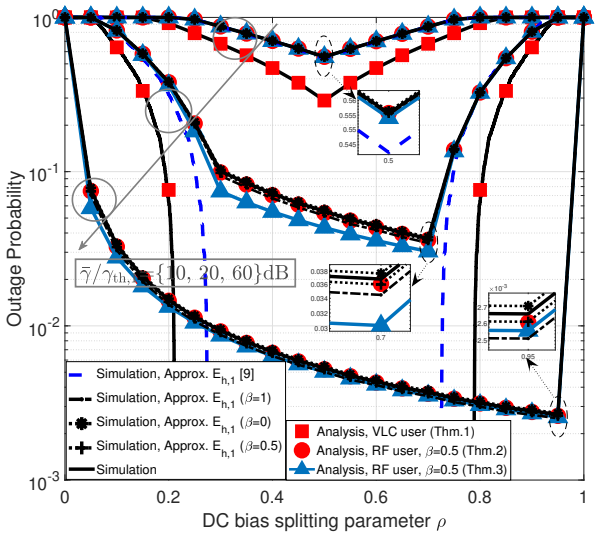

Fig. 5: Outage probability versus the DC bias splitting parameter ρ.

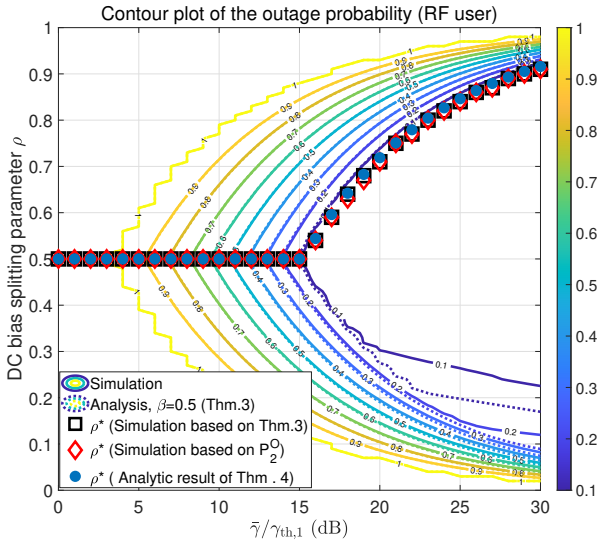

Fig. 6: The contour plot of the outage probability for RF user versus DC bias splitting parameter ρ and the normalized SNR $\bar{\gamma}/\gamma_{th,1}$(dB).

different normalized SNR, i.e., $\bar{\gamma}/\gamma_{th,1} = \{10, 20, 60\}$ dB, while fixing the ratio as $\bar{R} = 20$. Intuitively, the value of the DC bias $\mathcal{B}^*$ leading to the minimized outage probability of U_2 belongs in the range of $\rho \in [0.5, 1]$, equivalently $\mathcal{B}^*_{\mathrm{m}} \in [6, 12]$ mA, which is in line with the findings in [15]. Specifically, the optimal DC bias for the cases $\bar{\gamma}/\gamma_{th,1} = \{10, 20, 60\}$ dB can be set as $\rho = \{0.5, 0.7, 0.95\}$, respectively. Moreover, one can observe that the outage probability of U_1 is symmetric with respect to the $\rho = 0.5$, which is due to the impact of the peak amplitude $\mathcal{A}$, i.e., $\rho_A = \min(\rho, 1-\rho)$. Similarly, to further verify the effectiveness of the Theorem 2, it is noted that $N_{\mathrm{m}} = \{7, 14, 10\}$.

To obtain more insights of the SLIPT optimization, the suboptimal DC bias splitting parameter ρ^* leading to the minimum outage probability is investigated for different values of normalized SNR, i.e., $\bar{\gamma}/\gamma_{th,1}$. Thus, the following Fig.6 is depicted to reveal the mutual effects of ρ and $\bar{\gamma}/\gamma_{th,1}$ on the outage probability of the RF user, as well to verify the accuracy of Theorem 4. Moreover, the ratio is fixed as $\bar{R} = 20$. In Fig.6, apart from presenting the simulation results and analytical results given by Theorem 3 with $\beta = 0.5$, the universal search based on the exact P_2^{O} (as defined in (46)), the approximate $P_2^{\mathrm{O,app(c)}}$ (as given in Theorem 3), and the analytic solution provided by Theorem 4 are illustrated to obtain the minimum outage probability for U_2. In this figure, it is observed that the theoretical solution derived by Theorem 4 matches well with all other alternatives obtained from simulations. Moreover, one can find that larger SNR and the corresponding suboptimal DC bias splitting parameter can jointly result in the minimized outage probability of U_2. Meanwhile, the simulations are presented to further verify the accuracy of Theorem 3, by comparing the analytic performance achieved in Theorem 3 with $\beta = 0.5$ and simulation results. Along with the diverse normalized SNRs $\bar{\gamma}/\gamma_{th,1}$, the optimal DC splitting parameter ρ^* derived from the simulations belong to the range of $\rho^* \in [0.5, 1]$, which coincides well with the result of Proposition 2. Another intuitive observation is that the closed-form expression of ρ^* given by Theorem 4 fits well with the results by exhaustive search, especially from the outage probability in Theorem 3 and that of (46). This finding verifies the accuracy and effectiveness of Theorem 4.

VI. Conclusions

In this paper, we have investigated the cooperative hybrid VLC/RF relaying network which consists of a VLC user and an RF one, according to which, the information transmitted from the LED-based AP to the RF user can be facilitated. In order to preserve the energy sustainability of the proposed system, the simultaneous lightwave information and power transfer (SLIPT) strategy has been adopted. Meanwhile, a cognitive-based policy has been leveraged to perform adaptive resource allocation, according to which, the RF user solely utilizes the surplus resources, without affecting the performance of the VLC user. While considering that the users are randomly deployed, the performance of both users has been investigated in terms of outage probability. In specific, the outage probability of the VLC user has been derived in closed-from. Moreover, novel tractable bounds of the harvested energy have been introduced, which have been further used to derive the accurate approximate expression for the outage probability of the RF user, in terms of infinite but convergent series, as well as the corresponding closed-form one. Furthermore, the suboptimal DC bias that achieves the minimum outage probability for the RF user, has been derived, considering the constraints imposed by the cognitive-inspired resource allocation policy. Finally, numerical results have been presented to verify the accuracy of the proposed bounds for the harvested energy and the outage performance analysis, as well as the effectiveness of the DC bias optimization.

APPENDIX A
PROOF OF THEOREM 2

For notational brevity, the general expression of the outage probability for U_2 presented in (31) can be rewritten as

$$\mathrm{P}_2^{\mathrm{O}} = \mathrm{P}_{1,2}^{\mathrm{O}} + \mathrm{P}_{2,\mathrm{RF}}^{\mathrm{O}}, \tag{46}$$

in which the first term can be further derived by using (25) with $i = 2$, while the second term can be further denoted as

$$\mathrm{P}_{2,\mathrm{RF}}^{\mathrm{O}} = \mathrm{P}_{\mathrm{r}}\left[r_1 < r_{1,2}^c, |h_2|^2 < \frac{(2^{\frac{\mathrm{R}_{\mathrm{th},2}}{B_{\mathrm{r}}}} - 1)\sigma_2^2 G_{\mathrm{R}}}{E_{\mathrm{h},1}}\right]. \tag{47}$$

Moreover, by using the approximate expression for the harvested energy as given in (22), i.e., considering that $E_{\mathrm{h},1} \approx E_{\mathrm{h},1}^{\mathrm{app}*}$, $\mathrm{P}_{2,\mathrm{RF}}^{\mathrm{O}}$, which refers to the probability of the event that x_2 is decoded successfully at U_1 but not at U_2, can be approximated by

$$\begin{aligned}\mathrm{P}_{2,\mathrm{RF}}^{\mathrm{O,app}} &= \mathrm{P}_{\mathrm{r}}\Big[|h_2|^2 < \Lambda_c^* \left(r_1^2 + r_2^2 - 2r_1 r_2 \cos(\theta_2 - \theta_1)\right)^{\frac{v}{2}} \\ &\qquad \times (r_1^2 + L^2)^{\frac{(s+3)}{2}}, \quad r_1 < r_{1,2}^c\Big] \\ &= F_{|\mathrm{h}_2|^2}\Big(\Lambda_c^* \left(r_1^2 + r_2^2 - 2r_1 r_2 \cos(\theta_2 - \theta_1)\right)^{\frac{v}{2}} \\ &\qquad \times (r_1^2 + L^2)^{\frac{(s+3)}{2}}\Big),\end{aligned} \tag{48}$$

with the constraint of $r_1 < r_{1,2}^c$, where

$$\Lambda_{\mathrm{c}}^* = \frac{(2^{\frac{\mathrm{R}_{\mathrm{th},2}}{B_{\mathrm{r}}}} - 1)\sigma_2^2 (4\pi/\lambda)^2 d_0^{(2-v)}}{f\eta P_1 \mathcal{B} V_{\mathrm{t}} \mathcal{W}_{\mathrm{oc}} C(s+1) L^{(1+s)}}. \tag{49}$$

Moreover, assuming that the RF link suffers from Rician fading with factor K, the CDF of $|h_2|^2$ is [40]

$$\begin{aligned}F_{|\mathrm{h}_2|^2}(z) &= 1 - Q_1\left(\sqrt{2K}, \sqrt{\frac{2(1+K)z}{\Omega}}\right) \\ &\overset{(d)}{=} \exp(-K)\sum_{n=0}^{\infty}(-1)^n \frac{L_{\mathrm{n}}^{(0)}(K)}{\Gamma(n+2)}\left(\frac{(1+K)z}{\Omega}\right)^{n+1},\end{aligned} \tag{50}$$

where $Q_1(.,.)$ is the generalized Marcum $Q-$function [39]. Moreover, the above step (ds) is established by reffering to (8) in [39], which is given as

$$\begin{aligned}&Q_m(\alpha, \beta) = \\ &1 - \sum_{n=0}^{\infty}(-1)^n \exp(-\frac{\alpha^2}{2})\frac{L_{\mathrm{n}}^{(m-1)}(\frac{\alpha^2}{2})}{\Gamma(n+m+1)}\left(\frac{\beta^2}{2}\right)^{n+m},\end{aligned} \tag{51}$$

where $L_{\mathrm{n}}^{(m-1)}$ is the generalized Laguerre polynomial of degree n and order $(m-1)$, $\Gamma(.)$ denotes the gamma function which is defined via a convergent improper integral. Note that the absolute convergence of the series in (50) has been proved in [39], by utilizing the inequalities for Laguerre functions.

Considering the randomness of the location of U_1 and U_2, the outage probability of the users shall be evaluated in the form of expectation, with respect to the polar coordinate consisting of radial and angular variable. To this end, (48) can be rewritten as

$$\begin{aligned}\mathrm{P}_{2,\mathrm{RF}}^{\mathrm{O,app}} = \mathbb{E}\Big[F_{|\mathrm{h}_2|^2}\Big(&\Lambda_c^* \left(r_1^2 + r_2^2 - 2r_1 r_2 \cos(\theta_2 - \theta_1)\right)^{\frac{v}{2}} \\ &\times (r_1^2 + L^2)^{\frac{(s+3)}{2}}\Big)\Big], \quad r_1 < r_{1,2}^c.\end{aligned} \tag{52}$$

Based on the expectation operation on continues variables, i.e., r_1, r_2, and θ_1, θ_2, thus the outage probability, i.e., $\mathrm{P}_{2,\mathrm{RF}}^{\mathrm{O,app}}$, can be further derived by integrating the radial and angular variables with respect to the dedicated ranges, i.e., $\theta_i \in [0, 2\pi]$, $r_1 \in [0, r_{1,2}^c)$, and $r_2 \in [0, R_0]$. Moreover, by considering the PDF function of the radial and angular variable into calculating (52), we have

$$\begin{aligned}&\mathrm{P}_{2,\mathrm{RF}}^{\mathrm{O,app}} = \\ &\int_0^{R_0}\int_0^{r_{1,2}^c}\int_0^{2\pi}\int_0^{2\pi} F_{|\mathrm{h}_2|^2}\Big(\Lambda_c^* \left(r_1^2 + r_2^2 - 2r_1 r_2 \cos(\theta_2 - \theta_1)\right)^{\frac{v}{2}} \\ &\qquad \times (r_1^2 + L^2)^{\frac{(s+3)}{2}}\Big) f_{\Theta_1}(\theta_1) f_{\Theta_2}(\theta_2) f_{\gamma_1}(r_1) f_{\gamma_2}(r_2) \\ &\qquad \times d_{\theta_1}\, d_{\theta_2}\, d_{r_1}\, d_{r_2}.\end{aligned} \tag{53}$$

To this end, after substituting (48), (50), and (1), (2) into (53), $\mathrm{P}_{2,\mathrm{RF}}^{\mathrm{O,app}}$ can be eventually expressed by

$$\begin{aligned}\mathrm{P}_{2,\mathrm{RF}}^{\mathrm{O,app}} =& \exp(-K)\sum_{n=0}^{\infty}(-1)^n \frac{L_{\mathrm{n}}^{(0)}(K)}{\Gamma(n+2)}\left(\frac{(1+K)\Lambda_c^*}{\Omega}\right)^{(n+1)} \\ &\times \frac{1}{\pi^2 R_0^4}\underbrace{\int_0^{R_0}\int_0^{r_{1,2}^c}\int_0^{2\pi}\int_0^{2\pi} r_1 r_2 (r_1^2 + L^2)^{\frac{(s+3)(n+1)}{2}}}_{} \\ &\underbrace{\left(r_1^2 + r_2^2 - 2r_1 r_2 \cos(\theta_2 - \theta_1)\right)^{\frac{v(n+1)}{2}} d_{\theta_1}\, d_{\theta_2}\, d_{r_1}\, d_{r_2}}_{\Xi}.\end{aligned} \tag{54}$$

Inspired by the independent radial and angle variables in users' polar coordinates, the radial-based and angle-based integrals are combined by using the binomial expansion function, to further express Ξ as $\Xi = \sum_{p=0}^{\frac{(n+1)v}{2}} \binom{\frac{(n+1)v}{2}}{p} \Xi_r \Xi_\theta$, with Ξ_r and Ξ_θ being the expectation operation with respect to the radial and angular, respectively. Specifically,

$$\begin{aligned}\Xi_r = &\int_0^{R_0}\int_0^{r_{1,2}^c} r_1 r_2 (r_1^2 + L^2)^{\frac{(s+3)(n+1)}{2}} (r_1^2 + r_2^2) \\ &\times (-2r_1 r_2)^{(\frac{v(n+1)}{2} - p)} d_{r_1}\, d_{r_2},\end{aligned} \tag{55}$$

$$\Xi_\theta = \int_0^{2\pi}\int_0^{2\pi} \cos(\theta_2 - \theta_1)^{(\frac{v(n+1)}{2} - p)} d_{\theta_1}\, d_{\theta_2}. \tag{56}$$

Then, by using the binomial expansion to facilitate the corresponding integrals' calculation in (55) and (56) and referring to the integral of cosine function given in [13] and [32], thus

This article has been accepted for publication in a future issue of this journal, but has not been fully edited. Content may change prior to final publication. Citation information: DOI 10.1109/TCOMM.2021.3051908, IEEE Transactions on Communications

we can further obtain the following expressions in the closed form, as

$$\Xi_r = \sum_{l=0}^{p} \sum_{q=0}^{\frac{(n+1)(s+3)}{2}} \binom{p}{l} \binom{\frac{(n+1)(s+3)}{2}}{q} (-2)^{(\frac{v(n+1)}{2}-p)} L^{((s+3)(n+1)-2q)} \Big(\frac{(r_{1,2}^c)^M R_0^N}{MN}\Big) \tag{57}$$

and

$$\Xi_\theta = \sum_{k=0}^{\frac{(n+1)v}{2}-p} \binom{\frac{(n+1)v}{2}-p}{k} (-1)^{\frac{(n+1)v}{2}-p-k} \mathcal{J}^2. \tag{58}$$

To this end, by using (25) with $i = 2$ and plugging $\mathrm{P}_{2,\mathrm{RF}}^{\mathrm{O,app}}$ instead of $\mathrm{P}_{2,\mathrm{RF}}^{\mathrm{O}}$, the approximate outage probability of U_2 can be directly derived from (46) as in (32), which completes the proof.

Appendix B
Proof of Theorem 3

Considering (3.7) in [41], an immediate consequence of (51) is that when $\beta \to 0^+$, the m-th order Marcum Q-function, i.e., $Q_m(\alpha, \beta)$, can be approximated as

$$Q_m(\alpha, \beta) = 1 - \frac{\beta^{2m}}{2^m m!} \exp(-\frac{\alpha^2}{2}). \tag{59}$$

In such case, recalling to the variable of function $F_{|\mathrm{h}_2|^2}(z)$ shown in (48), the CDF of $|h_2|^2$ can be approximately expressed as follows after substituting (59) into (50) with assuming $z \to 0^+$, that is

$$\begin{aligned} F_{|\mathrm{h}_2|^2}(z) &= 1 - Q_1\left(\sqrt{2K}, \sqrt{\frac{2(1+K)z}{\Omega}}\right) \\ &\approx \frac{(1+K)z}{\Omega} \exp(-K). \end{aligned} \tag{60}$$

In turn, the outage probability of U_2 (48) can be further calculated using the Q-function (60), thus, we have

$$\begin{aligned} \mathrm{P}_{2,\mathrm{RF}}^{\mathrm{O,app}} \approx \left(\frac{(1+K)\Lambda_c^*}{\Omega}\right) \exp(-K)(r_1^2 + L^2)^{\frac{(s+3)}{2}} \\ \times \left(r_1^2 + r_2^2 - 2r_1 r_2 \cos(\theta_2 - \theta_1)\right)^{\frac{v}{2}}. \end{aligned} \tag{61}$$

Since U_1 and U_2 are uniformly distributed in the disc, the expectation of the outage probability for U_2 can be obtained using Ξ presented in (54), given as

$$\mathrm{P}_{2,\mathrm{RF}}^{\mathrm{O,app}} = \left(\frac{(1+K)\Lambda_c^*}{\Omega}\right) \exp(-K) \frac{\Xi}{\pi^2 R_0^4}. \tag{62}$$

Recalling the outage probability for U_2, a closed form approximation for the outage probability of U_2 can be presented as

$$\begin{aligned} \mathrm{P}_2^{\mathrm{O,app}} \approx \mathrm{P}_{1,2}^{\mathrm{O}} + \sum_{p=0}^{\frac{(n+1)v}{2}} \binom{\frac{(n+1)v}{2}}{p} \left(\frac{(1+K)\Lambda_c^*}{\Omega}\right) \\ \times \exp(-K) \frac{\Xi_r \Xi_\theta}{\pi^2 R_0^4}, \end{aligned} \tag{63}$$

with the terms Ξ_r and Ξ_θ being the integral operations of radial and angle, which are given in (57) and (58), respectively. Consequently, an approximate expression for the outage probability of U_2 can be achieved by substituting (25) ($i = 2$), (57), and (58) into (63), and thus the proof is completed.

Appendix C
Proof of Proposition 1

Considering that the best outage performance for VLC user can be obtained when there is no outage occurring, we have

$$\mathcal{R}_{1,1} \geqslant \mathrm{R}_{\mathrm{th},1}, \tag{64}$$

where $\mathcal{R}_{1,1}$ is the achievable rate of decoding x_1 at U_1, as given in (14). Moreover, considering the proposed cognitive-based resource allocation policy, the information transmission to U_1 shall make full use of the resources allocated to the VLC link, if needed. Accordingly, the inequality given by (64) can be rewritten as

$$\mathcal{R}_1 \geqslant \mathrm{R}_{\mathrm{th},1}. \tag{65}$$

To this end, by substituting the achievable rate given by (13) in (65) and after some mathematical manipulations, the coefficient ρ related to the DC component can be decided by

$$[\min(\rho, 1-\rho)]^2 \geqslant \frac{2\pi\sigma_1^2 \left(2^{\mathrm{R}_{\mathrm{th},1}/B_{\mathrm{v}}} - 1\right)}{e\left[\eta P_1 (I_{\mathrm{H}} - I_{\mathrm{L}}) h_1\right]^2}. \tag{66}$$

Regarding h_1 which is defined in (5), it is recalled that considering the constraint $r_1 \in [0, R_0]$, its range is determined by (7). So far, the inequality (66) can always be true when $h_1 = h_{1,\min}$. To this end, the right term in (66) can be eventually expressed as that given in (40), thus, we have

$$\min(\rho, 1-\rho) \geqslant \rho_{\mathcal{A},L}. \tag{67}$$

This result implies that when the value of ρ satisfies the inequality in (67), the resource allocation inspired by the cognitive policy can help to facilitate realizing the non-outage status of U_1, which completes the proof of the first case in Proposition 1.

By observing $\rho_{\mathcal{A},L}$ given in (38) and (40), one can see that when $\rho_{\mathcal{A},L} > 0.5$, zero-tolerance requirement of the outage events occurring at the VLC user is infeasible, due to the constraint of ρ, i.e., $\rho \in [0, 1]$. Under such assumption, the minimum outage probability of U_1 should be further explored by referring to (25) with $i = 1$, which can be transformed to an univariate expression with respect to ρ, expressed as

$$\begin{aligned} \mathrm{P}_{1,1}^{\mathrm{O}}(\rho) = 1 + \frac{L^2}{R_0^2} - [\min(\rho, 1-\rho)]^{\frac{2}{3+s}} \\ \times \frac{\left[e^2(\eta P_1)(I_{\mathrm{H}} - I_{\mathrm{L}}) C (s+1) L^{(s+1)}\right]^{\frac{2}{3+s}}}{R_0^2 \left[2\pi\sigma_1^2 (2^{\frac{\mathrm{R}_{\mathrm{th},1}}{B_{\mathrm{v}}}} - 1)\right]^{\frac{1}{3+s}}}. \end{aligned} \tag{68}$$

Note that the optimal outage probability, namely the minimum value of (68) can be achieved when $\rho^* = 0.5$ for the case 2 of Proposition 1.

To this end, Proposition 1 is deduced, which completes the proof and its corresponding discussion.

APPENDIX D
PROOF OF THEOREM 4

Inspired by the priority in serving U_1, we have already found out that whether the non-outage status of U_1 can be reached is determined by the value of $\rho_{\mathcal{A},L}$, as shown in Proposition 1. In short, the variable ρ shall be designed to meet the best outage performance of U_1. To this direction, two observations need to be considered: i) one is that the optimal value $\rho^* = 0.5$ can be decided when $\rho_{\mathcal{A},L} > 0.5$, corresponding to the case 2 in Proposition 1, which still holds the outage probability with $\mathrm{P}_{1,1}^{\mathrm{O}} \neq 0$, ii) another with $\rho_{\mathcal{A},L} \leq 0.5$ denotes the case that there is non-outage for U_1, thus the optimal DC bias is only designed to reach the minimum outage probability for U_2, which is mainly discussed in the following.

Considering the approximated outage probability for U_2 being as a function of ρ, given by (36), one can observe that the outage probability for U_2 mainly depends on the outage event decoding signal x_2 at U_1, while considering the assumption in Theorem 3, i.e., $\Lambda_c^* \to 0^+$. To this end, a general discussion about the optimization problem can be divided into two cases. For a specific value of $r_{1,2}^c$, given by (30), it holds that

- If $r_{1,2}^c \leq R_0$, the outage events for decoding information x_2 at U_1 via the VLC link may occur. Also, considering the approximation assumed in Theorem 3, thus we have

$$\begin{aligned}\mathrm{P}_2^{\mathrm{O,app(c)}} &\approx \mathrm{P}_{1,2}^{\mathrm{O}} \\ &= 1 - \frac{\left((C(s+1)L^{(s+1)})^2/\zeta_{1,2}^*\right)^{\frac{1}{3+s}} - L^2}{R_0^2}.\end{aligned} \tag{69}$$

- If $r_{1,2}^c > R_0$, there is no outage for decoding x_2 via the VLC link, thus the outage probability for U_2 can be expressed as

$$\begin{aligned}\mathrm{P}_2^{\mathrm{O,app(c)}} &\approx \mathrm{P}_{2,\mathrm{RF}}^{\mathrm{O}} \\ &\approx \left(\frac{(1+K)\Lambda_c^*}{\Omega}\right)\exp(-K)\frac{\Xi_r \Xi_\theta}{\pi^2 R_0^4}.\end{aligned} \tag{70}$$

To this end, the optimization problem given by (43) can be eventually rewritten as

$$\begin{aligned}&\min_{\rho}\ \mathrm{P}_2^{\mathrm{O,app(c)}} \\ &\mathbf{s.t.}\ \mathrm{C}_1,\ \mathrm{C}_2^{'},\end{aligned} \tag{71}$$

where $\mathrm{P}_2^{\mathrm{O,app(c)}}$ is decided by (69) and (70) based on above two cases. Accordingly, the optimum solution of ρ to (71) can be discussed by

- If $r_{1,2}^c \leq R_0$, By observing that $\zeta_{1,2}^*$ is a decreasing function of ρ within the range of $\rho \in [0.5, 1]$, it is evident that $\rho^* = 0.5$.
- If $r_{1,2}^c > R_0$, the corresponding approximate expression for $\mathrm{P}_2^{\mathrm{O,app(c)}}$ is decreasing with $\rho \in [0.5, 1]$. This finding can be explored by considering the behavior of Λ_c^* and Ξ_r with respect to ρ.

Evidently, under the aforementioned assumptions, the approximate outage probability is decided by choosing either (69) or (70), according to the value of $r_{1,2}^c$. More specifically, it's necessary to recall that we assume that the value of (70) is much smaller than that of (69). Till now, min-max criteria can be applied to minimize the outage probability of U_2. To this end, the suboptimal ρ leading to the minimum outage probability of U_2 can be yielded when $r_{1,2}^c = R_0$, from which we can derive the suboptimal $\rho_{\mathcal{A}}^*$ as given in (45), while the corresponding DC splitting parameter can be expressed as (44).

Consequently, it's intuitive to find that the value of $\rho_{\mathcal{A}}^*$ given in (45) is larger than $\rho_{\mathcal{A},L}$. That is to say, when $\rho_{\mathcal{A}}^*$ is chosen, there is definitely no outage occurred for the VLC user, which satisfies the requirement of $\mathrm{P}_{1,1}^{\mathrm{O}} = 0$ as well as the constraint C_1 shown in (41). To this end, while considering both cases presented in Proposition 1, the proof is completed.

REFERENCES

[1] Z. Ma, Z. Zhang, Z. Ding, P. Fan, and H. Li, "Key techniques for 5G wireless communications: Network architecture, physical layer, and MAC layer perspectives," *Sci. China Inf. Sci.*, vol. 58, no. 4, pp. 1–20, Apr 2015.

[2] Z. Zhang, Y. Xiao, Z. Ma, M. Xiao, Z. Ding, X. Lei, G. K. Karagiannidis, and P. Fan, "6G wireless networks: Vision, requirements, architecture, and key technologies," *IEEE Veh. Technol. Mag.*, vol. 14, no. 3, pp. 28–41, 2019.

[3] M. Ayyash, H. Elgala, A. Khreishah, V. Jungnickel, T. Little, S. Shao, M. Rahaim, D. Schulz, J. Hilt, and R. Freund, "Coexistence of WiFi and LiFi toward 5G: concepts, opportunities, and challenges," *IEEE Commun. Mag.*, vol. 54, no. 2, pp. 64–71, 2016.

[4] M. A. Khalighi and M. Uysal, "Survey on free space optical communication: A communication theory perspective," *IEEE Commun. Surveys Tuts.*, vol. 16, no. 4, pp. 2231–2258, 2014.

[5] H. Kim, D. Kim, S. Yang, Y. Son, and S. Han, "Mitigation of inter-cell interference utilizing carrier allocation in visible light communication system," *IEEE Commun. Lett.*, vol. 16, no. 4, pp. 526–529, 2012.

[6] "IEEE standard for local and metropolitan area networks–part 15.7: Short-range wireless optical communication using visible light," *IEEE Std 802.15.7-2011*, pp. 1–309, 2011.

[7] P. Shams, M. Erol-Kantarci, and M. Uysal, "MAC layer performance of the IEEE 802.15.7 visible light communication standard," *Trans Emerging Tel Tech.*, vol. 27, no. 5, pp. 662–674, 2016.

[8] G. Pan, P. D. Diamantoulakis, Z. Ma, Z. Ding, and G. K. Karagiannidis, "Simultaneous lightwave information and power transfer: Policies, techniques, and future directions," *IEEE Access*, vol. 7, pp. 28 250–28 257, 2019.

[9] T. Rakia, H. Yang, F. Gebali, and M. Alouini, "Optimal design of dual-hop VLC/RF communication system with energy harvesting," *IEEE Commun. Lett.*, vol. 20, no. 10, pp. 1979–1982, 2016.

[10] X. Zhou, S. Li, H. Zhang, Y. Wen, Y. Han, and D. Yuan, "Cooperative NOMA based VLC/RF system with simultaneous wireless information and power transfer," in *Proc. IEEE/CIC Int. Conf. Commun. China (ICCC)*, 2018, pp. 100–105.

[11] V. K. Papanikolaou, P. D. Diamantoulakis, and G. K. Karagiannidis, "User Grouping for Hybrid VLC/RF Networks with NOMA: A Coalitional Game Approach," *IEEE Access*, pp. 1–1, 2019.

[12] V. K. Papanikolaou, P. P. Bamidis, P. D. Diamantoulakis, and G. K. Karagiannidis, "Li-Fi and Wi-Fi with common backhaul: Coordination and resource allocation," in *2018 IEEE Wireless Communications and Networking Conference (WCNC)*, Apr. 2018, pp. 1–6.

[13] Y. Xiao, P. D. Diamantoulakis, Z. Fang, Z. Ma, L. Hao, and G. K. Karagiannidis, "Hybrid lightwave/rf cooperative NOMA networks," *IEEE Trans. Wireless Commun.*, vol. 19, no. 2, pp. 1154–1166, 2020.

[14] "Status of IEEE 802.11 light communication TG," http://www.ieee802.org/11/Reports/tgbb_update.htm, accessed: 2020-08-04.

[15] P. D. Diamantoulakis, G. K. Karagiannidis, and Z. Ding, "Simultaneous lightwave information and power transfer (SLIPT)," *IEEE Trans. Green Commun. and Netw.*, vol. 2, no. 3, pp. 764–773, 2018.

[16] P. D. Diamantoulakis and G. K. Karagiannidis, "Simultaneous lightwave information and power transfer (SLIPT) for indoor IoT applications," in *GLOBECOM 2017 - 2017 IEEE Global Communications Conference*, 2017, pp. 1–6.

[17] R. Zhang and C. K. Ho, "MIMO broadcasting for simultaneous wireless information and power transfer," *IEEE Trans. Wireless Commun.*, vol. 12, no. 5, pp. 1989–2001, 2013.

[18] Z. Wang, D. Tsonev, S. Videv, and H. Haas, "On the design of a solar-panel receiver for optical wireless communications with simultaneous energy harvesting," *IEEE J. Sel. Areas Commun.*, vol. 33, no. 8, pp. 1612–1623, 2015.

[19] J. Fakidis, S. Videv, S. Kucera, H. Claussen, and H. Haas, "Indoor optical wireless power transfer to small cells at nighttime," *J. Lightw. Technol.*, vol. 34, no. 13, pp. 3236–3258, 2016.

[20] Z. Wang, D. Tsonev, S. Videv, and H. Haas, "Towards self-powered solar panel receiver for optical wireless communication," in *2014 IEEE International Conference on Communications (ICC)*, 2014, pp. 3348–3353.

[21] I. Krikidis, S. Timotheou, S. Nikolaou, G. Zheng, D. W. K. Ng, and R. Schober, "Simultaneous wireless information and power transfer in modern communication systems," *IEEE Commun. Mag.*, vol. 52, no. 11, pp. 104–110, 2014.

[22] Z. Ding, I. Krikidis, B. Sharif, and H. V. Poor, "Wireless information and power transfer in cooperative networks with spatially random relays," *IEEE Trans. Wireless Commun.*, vol. 13, no. 8, pp. 4440–4453, 2014.

[23] T. Rakia, H. Yang, F. Gebali, and M. Alouini, "Dual-hop VLC/RF transmission system with energy harvesting relay under delay constraint," in *Proc. IEEE Globecom Workshops (GC Wkshps)*, 2016, pp. 1–6.

[24] G. Pan, J. Ye, and Z. Ding, "Secrecy outage analysis of hybrid VLC-RF systems with light energy harvesting," in *2017 IEEE 18th International Workshop on Signal Processing Advances in Wireless Communications (SPAWC)*, 2017, pp. 1–5.

[25] M. R. Zenaidi, Z. Rezki, M. Abdallah, K. A. Qaraqe, and M. Alouini, "Achievable rate-region of VLC/RF communications with an energy harvesting relay," in *GLOBECOM 2017 - 2017 IEEE Global Communications Conference*, 2017, pp. 1–7.

[26] H. Tran, G. Kaddoum, P. D. Diamantoulakis, C. Abou-Rjeily, and G. K. Karagiannidis, "Ultra-small cell networks with collaborative RF and lightwave power transfer," *IEEE Trans. Commun.*, vol. 67, no. 9, pp. 6243–6255, 2019.

[27] M. Matin, *Spectrum Access and Management for Cognitive Radio Networks*, 1st ed. Springer Publishing Company, Incorporated, 2016.

[28] A. Goldsmith, S. A. Jafar, I. Maric, and S. Srinivasa, "Breaking spectrum gridlock with cognitive radios: An information theoretic perspective," *Proc. IEEE*, vol. 97, no. 5, pp. 894–914, 2009.

[29] P. D. Diamantoulakis, K. N. Pappi, S. Muhaidat, G. K. Karagiannidis, and T. Khattab, "Carrier aggregation for cooperative cognitive radio networks," *IEEE Trans. Veh. Technol*, vol. 66, no. 7, pp. 5904–5918, 2017.

[30] M. Hammouda, J. Peissig, and A. M. Vegni, "Design of a cognitive vlc network with illumination and handover requirements," in *2017 IEEE International Conference on Communications Workshops (ICC Workshops)*, 2017, pp. 451–456.

[31] N. Varshney and A. K. Jagannatham, "Cognitive decode-and-forward MIMO-RF/FSO cooperative relay networks," *IEEE Commun. Lett.*, vol. 21, no. 4, pp. 893–896, 2017.

[32] G. Pan, J. Ye, and Z. Ding, "Secure hybrid VLC-RF systems with light energy harvesting," *IEEE Trans. Commun.*, vol. 65, no. 10, pp. 4348–4359, 2017.

[33] M. Alouini and A. J. Goldsmith, "Area spectral efficiency of cellular mobile radio systems," *IEEE Trans. Veh. Technol.*, vol. 48, no. 4, pp. 1047–1066, 1999.

[34] L. Yin, W. O. Popoola, X. Wu, and H. Haas, "Performance evaluation of non-orthogonal multiple access in visible light communication," *IEEE Trans. Commun.*, vol. 64, no. 12, pp. 5162–5175, 2016.

[35] J. M. Kahn and J. R. Barry, "Wireless infrared communications," *Proc. IEEE*, vol. 85, no. 2, pp. 265–298, 1997.

[36] A. Chaaban, Z. Rezki, and M. Alouini, "On the capacity of the intensity-modulation direct-detection optical broadcast channel," *IEEE Trans. Wireless Commun.*, vol. 15, no. 5, pp. 3114–3130, 2016.

[37] Chengliu Li, Wenyan Jia, Quan Tao, and Mingui Sun, "Solar cell phone charger performance in indoor environment," in *2011 IEEE 37th Annual Northeast Bioengineering Conference (NEBEC)*, 2011, pp. 1–2.

[38] A. P. Prudnikov, Y. A. Brychkov, and O. I. Marichev, *Integrals and Series*. CRC Press, 1992.

[39] S. Andras, A. Baricz, and Y. Sun, "The generalized marcum Q-function: an orthogonal polynomial approach," *arXiv:1010.3348*, 2010.

[40] M. Simon and M. Alouini, *Digital Communication over Fading Channels*. Wiley, 2005.

[41] X. Li, "Asymptotic performance analysis for EGC and SC over arbitrarily correlated Nakagami-m fading channels," *University of British Columbia*, 2011.